Remote Sensing and Machine Learning based Optimization of Erosion in Ghizer District-Hindukush Using RUSLE and Hypsometric Modeling

Hafsa Batool[1], Maira Malik[1], Hafsa Asad[1], Syed Arsalan Bukhari[1], Rukhsar Shahzadi[1], Minahil Afzal[1], Saif Ullah Akhter[2]
[1]Instiute of Space Science, University of the Punjab, Lahore
[2]Department of Geography, Government Associate College, Eminabad, Gujranwala
*__Correspondence__: hafsa.batool@gmail.com

Citation | Batool. H, Malik. M, Asad. H, Bukhari. S. A, Shahzadi. R, Afzal. M, Akhter. S. U, "Remote Sensing and Machine Learning based Optimization of Erosion in Ghizer District-Hindukush Using RUSLE and Hypsometric Modeling, FCSI, Vol. 3 Issue. 4 pp 226-240, Dec 2025

Received| Nov 22, 2025 **Revised|** Dec 23, 2025 **Accepted|** Dec 24, 2025 **Published|** Dec 25, 2025.

Soil erosion-induced land degradation is now considered one of the most severe challenges of the 21st century, with acute risks to soil fertility, food security, human well-being, and global ecosystems. The objective of this study is to conduct a quantitative mapping of soil loss within the Ghizer district of Pakistan. To estimate soil loss in the region, the Revised Universal Soil Loss Equation (RUSLE) model was employed in conjunction with Remote Sensing (RS) and Geographic Information System (GIS) techniques. Analysis of the topographical characteristics of the study area reveals heightened vulnerability to soil loss, with the highest average annual soil loss recorded at 74 tons per hectare per year. The generated maps illustrate that the area exhibits the highest sediment yield of 246 tons per hectare per year, with an elevated average annual soil loss of 435 tons per year. The distribution across severity classes indicates 7% under the very high category, 14% under high, 18% under moderate, 10% under low, and 12% under very low soil loss categories within the Ghizer district. The results of this research help develop a rich information source for researchers and planners to develop more effective approaches for reducing soil loss within high-severity zone categories. Recommendations include the implementation of tree plantation initiatives and the construction of structures such as check dams, which have demonstrated effectiveness in controlling the process of soil erosion. Hypsometric Integrals (HIs) are estimated from empirical formulae based on the geographical plots of the measured contour elevation and the area they encompass. This study aims to calculate hypsometric integral values for the Ghizer River and its sub-watersheds in Hindukush using four different techniques and to compare the procedural techniques of its estimation and relevance to the erosion status. The hypsometric integral expresses precisely the ratio of relief elevation; it is not so cumbersome to use and can be computed easily within an RS environment.

Keywords: RUSLE, RS, ML, R factor, K factor, LS factor, C factor, P factor, HI.

Introduction:

The 20th century saw a significant increase in soil erosion, which is responsible for around 85% of land degradation worldwide. The author in [1] revealed that the greatest amount of this deterioration happened after World War II, which resulted in a notable 17% decline in agricultural output. With accuracy and consistency, modeling provides a methodical and numerical way to anticipate soil sedimentation and soil erosion yield in various environmental circumstances [2]. Significant problems caused by soil erosion include siltation in reservoirs and sediment accumulation in canals and rivers, which increases the likelihood of floods [3]. Additionally, reservoir disruption caused by silt deposition in watercourses shortens reservoir lifespans and increases maintenance costs [4]. Food production, highland ecosystems, and the local economy are all directly impacted by this occurrence [5].

More tropical-friendly than its earlier version, dating back to 1997, though originally developed to forecast water erosion in temperate countries, the Revised Universal Soil Loss Equation (RUSLE) offers a greater scope as it is an improvement on the Universal Soil Loss Equation (USLE). According to Wischmeier and Smith in 1978, RUSLE has wider parameters because it has data that were out of reach when USLE was first conceived. RUSLE is designed to be applied at the runoff plot or individual hillslope scale. It makes it easier to estimate an average of annual soil erosion rates for a given site in a variety of scenarios, including different cropping systems, management strategies, and erosion control measures. According to Garde and Kathyari in 1990, RUSLE also enables the projection of erosion rates in ungauged catchments when information on catchment parameters and local hydro-climatic variables is available. The highest rate of soil erosion that is acceptable and yet maintains commercial crop output is then shown by comparing these erosion projections with the region's known soil-loss tolerance (T) values. Because a field might have an endless number of slope lengths, RUSLE makes it possible to calculate erosion over multiple slope lengths. The erosion rate of a field can then be calculated by weighting the findings by the area of interest that each slope length represents. RUSLE enables extrapolation of the rate of erosion to determine the general pattern of erosion throughout a whole watershed by combining data from sample fields [6].

Hypsometry, the distribution of elevations, provides yet another useful technique by which to estimate rates of uplift and erosion across a landscape, and also by which to ascertain whether a landform has been predominantly produced through glacial or fluvial processes. Research by [7][8][9][10][11][12] all used this analytical technique [13]. According to Strahler's definition in 1952, he says that hypsometry is the measurement of. According to [14][15], the hypsometric integral (HI) relates to an erosion profile of the land surface below the hypsometric curve (HC). Since early times (since the 2nd half of the 20th century), HC has been used to describe and explain neo-tectonic events by indicating phases of erosion and sedimentation, catchment regions under study, geomorphic characteristics, and changes of landscape features. As essential instruments for hypsometric analysis, HIs and HCs provide information on landform development phases, topographic erosion, and surface roughness.

The HI has found formidable applications in the fields of geology, hydrology, tectonics, climatology, geomorphology, and glaciology, and its significance has been emphasized by the works of Lifton and Chase (1992), Masek et al. (1994), and Walcott and Summerfield (2008. Formulations by Ohmori (1993), Perez-Pena et al., 2009; and Mahmood and Gloaguen (2011 are commonly used to determine the hypsometric index.

$$HI = \frac{H_{\text{mean}} - H_{\text{min}}}{H_{\text{max}} - H_{\text{min}}}$$

The region's lowest, maximum, and average altitudes are shown by the symbols H_{min}, H_{max}, and H_{mean}, respectively. We define 'a' as the area below 'h', following the approach of [9][12]. As a result, we apply the following formula to obtain the Hypsometric Integral (HI):

$$HI = \frac{1}{n}\sum_{i=1}^{n} h_i'$$

Study Area:

The study area is Northern Pakistan; the district's center is Ghizer. Ghizer district, encapsulated in the glorious Himalayan mountain range, features a very diverse and not uncommon tectonic setting that built its geological terrain millions of years ago. The district's rich collection of geologic structures and structural characteristics is the result of continuous tectonic interactions between the Indian and Eurasian plate boundaries, where they collide. Shear zones, thrust faults, and folds are just a few of the geological structures that have formed as a result of this active tectonic environment. The MMT marks a region of strong seismic activity and tectonic activity that separates the Asian and Indian plates, and the study area is the sandwich zone in between the Karakoram Fault (KF) and Main Karakoram Thrust (MKT).

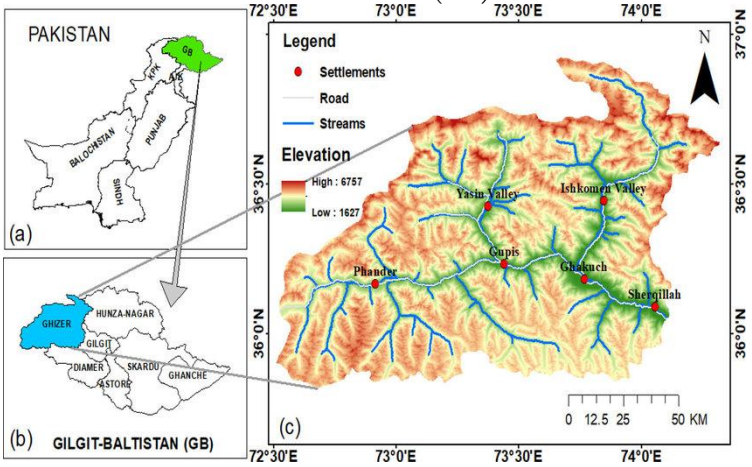

Figure 1. The study area Location [16]

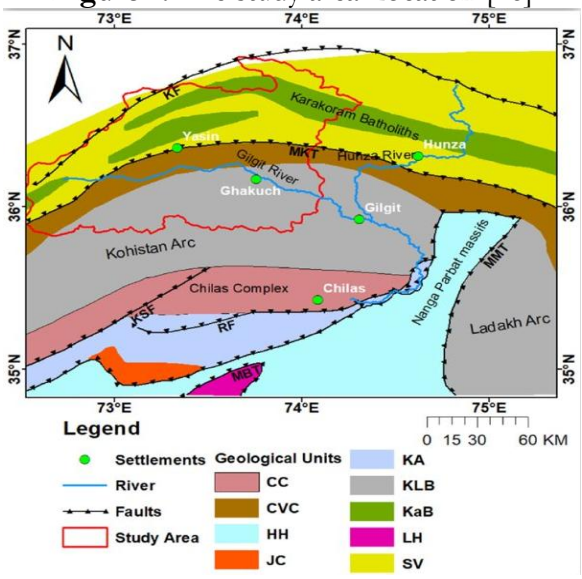

Figure 2. Geotectonic map of the Study area nd sub-urbs [16]

The RUSLE model's implementation in Ghizer District sheds important light on the soil erosion rates in various landforms and land use scenarios. A thorough evaluation of the possibility of soil loss is made easier by the RUSLE model, which incorporates cover management, conservation techniques, slope length and steepness, rainfall erosivity, and soil erodibility. Understanding erosion rates is vital for sustainable land management in Ghizer, where agriculture is the main industry, and land use techniques include terraced farming on

slopes by grazing fields, and wooded regions. Policymakers and land managers may use the RUSLE model to pinpoint areas of erosion risk, rank conservation efforts, and put specific policies in place to reduce soil erosion and maintain soil fertility.

Hypsometry, a study of the distribution of land surface height within a certain area, provides further context for understanding Ghizer District's geomorphological features. Hypsometric analysis reveals the morphometric features of the terrain, such as the distribution of the highlands, valleys, and slopes, by examining elevation data and topographical profiles. Hypsometry at Ghizer, the meeting point of the massive Hindu Kush and Karakoram mountain ranges, displays the predominance of high-altitude topography and the complex network of valleys sculpted over millennia by glaciers and rivers. To know the hypsometry of the Ghizer district, it is essential to understand erosion patterns because height gradients affect the dynamics of runoff, the movement of sediments, and the susceptibility of erosion at various altitudes and landforms.

Material and Methods:

Data Set:

Some of the critical factors that determine soil erosion are topography, climate, soil quality, precipitation, and LULC. The following useful datasets were used to assess the effect. Datasets from Landsat 8, Sentinel 2, and MODIS from Google Earth Engine were used to describe the study area. The derivation of the LS factor utilized the SRTM Digital Elevation Model at a spatial resolution of 30 m.

Table 1. Details on the data sources, availability, spatial resolution, and providers of datasets to obtain RUSLE (Revised Universal Soil Loss Equation) factors [17]

Sr. No.	Datasets	Dataset Provider	Dataset Availability	Spatial Resolution	Used for
1	Climate Hazards Group InfraRed Precipitation with Station (CHIRPS Pentad, Version 2.0 Final)	UCSB/CHG	From: 1981-01-01	0.05°	R factor
2	Open Land Map Soil Texture Class (USDA System)	EnvironmetriX Ltd	1950-01-01 – 2018-01-01	250 m	K factor
3	NASA SRTM Digital Elevation	NASA/USGS/JPL-Caltech	2000-02-11 – 2000-02-22	1 arcsec	LS factor
4	Sentinel-2 MSI, Level-1C	European Union / ESA / Copernicus	From: 2015-06-23	10 m	C factor
5	MODIS Land Cover Type Yearly Global 5	NASA LP DAAC (USGS EROS Center)	From: 2001-01-01	500 m	P factor

The Ghizer district soil erosion was evaluated using a hybrid methodology that used the RUSLE model with spectral indices. Both the qualitative and quantitative components of erosion evaluation were covered by this integrated technique. While the RUSLE model, well-known for its ease of use and broad application, provided a thorough quantitative examination of soil erosion, spectral indices gave qualitative insights into regions that were prone to erosion. The RUSLE model was improved by utilizing the vast amount of satellite data made accessible by GEE, as well as remote sensing and GIS capabilities [18]. This allowed for a comprehensive assessment of the dynamics of water erosion over the whole research region.

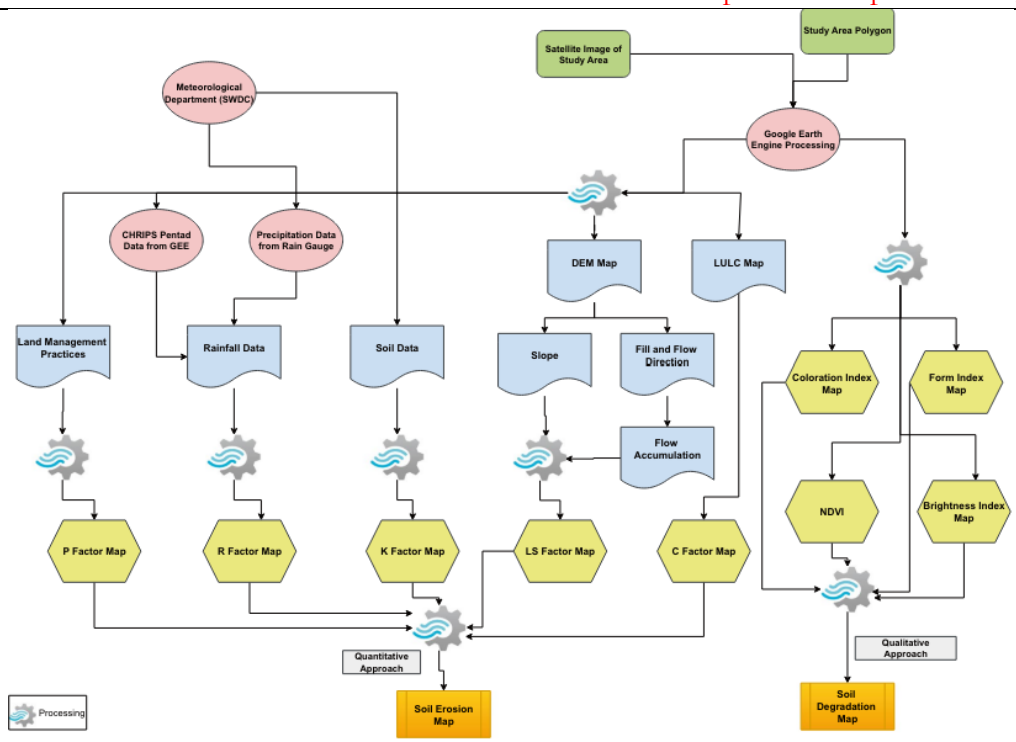

Figure 3. Flow chart for GEE-based computations [17]

RUSLE Model Application:

Soil erosion may be thoroughly evaluated with the techniques of RS-GIS and the RUSLE technique integrated [19]. The five-factor computation that is included in the RUSLE model is mathematically captured in Eq. 1, which improves consistency and accuracy when evaluating erosion in the accumulation environment.

$$A = R \times LS \times K \times P \times C \quad (1)$$

Where R is the rainfall (runoff) erosivity factor, LS is the slope length and steepness factor, K is the soil erodibility factor, P is the support practice factor, and C is the cover factor, then A is the average annual soil loss over a given time.

Rainfall Erosivity Factor (R):

The R factor, on the other hand, determines how rainfall affects erosion by estimating the input of these through rill and sheet erosion. A modified Method of Rango and Arnoldus (1987) was used to estimate the R factor. In this approach, annual erosivity is estimated where monthly as well as annual rainfall data are available. Eq. 2 was utilized in this work to determine the R factor based on rainfall data analysis.

$$log\ R = 1.69 \times (2) \sum(Pi2/P) + 1.29 \quad (2)$$

Rainfall (mm) is represented by the letters P, Pi, which stands for yearly rainfall (mm), and R for the erosivity factor.

Soil Erodibility Factor (K)

Soil erodibility is a factor that represents the soil's susceptibility to erosion and sedimentation under specific rainfall conditions, if not eroded very deeply. The erodibility factor is given by soil texture. The K value of silt is greatest, but the K value of sandy and coarse-loamy soils is moderate to low because of their greater rates of infiltration, which decrease runoff and lessen the likelihood of sediment transport. Conversely, clay possesses a low K value due to its difficulty in detaching. Eq. 3 is used to reclassify the soil map according to the K value. A lower K value denotes less soil erosion. The K value can range from zero to one.

$$K = 26.67 \times x1.14 \times 10{-}8 \times (12 - \alpha) + 0.0043 \times (\beta - 2) + 0.0033 \times (\gamma - 3) \quad (3)$$

Let x be defined as the proportion of clay particles less than the percentage of silt and very tiny sand grains multiplied by 100.

Let α stand for the fraction of organic particles.

Let β be the structural code, where proper particulate is indicated by some 1, fair particulate by several 2, somewhat particulate by some 3, and solid particulate by many 4.

Let γ be the code for the permeability profile, with -1 meaning extremely fast, -2 meaning medium to fast, -3 meaning medium, -4 meaning medium to slow, -5 meaning slow, and -6 meaning very slow.

Topographic Factor (LS):

Slope length, or the distance from the beginning point of water flow to the point at which the slope becomes sufficiently gentle for sediment deposition, is another topographical factor. Longer slopes result in greater soil loss from erosion, but slope steepness has a greater effect on erosion than slope length.

$$LS = (\text{Flow accumulation} \times \text{Grid size} / 22.1)^{0.4} \times (\text{Sin(slope)} \times 0.01745 / 0.09)^{1.4} \quad (4)$$

Cover Factor (C):

This factor is also a vital reduction factor, which represents how soil erosion is influenced by crop management practices. Determining factors are the type of crop/vegetation, percentage of cover, and stage of development. The regression equation related to the cover factor is shown in Eq. 5.

$$C = 1.01–1.2 \times NDVI \quad (5)$$

Support Practice Factor (P):

The favorable impacts of support practices on lowering soil erosion are reflected in the support practice factor (P), also known as the conservation practice factor. Under the regulations for agricultural land management, this component has a range of 0 to 1. Effective conservation practices are indicated by a value close to zero, whereas ineffective conservation activities are indicated by a value close to one.

Land Use Land Cover (LULC):

Short revisit times, high temporal resolution, and rich spectral configurations render Landsat-8 (L-8) and Sentinel-2 (S-2) products ideal for source extraction features in time series applied to medium-resolution satellite imagery. Moreover, time series-based pattern analysis of satellite imagery interprets the assimilation of information on spectral variations and the derived spectral–temporal metrics along with a wider pool of features used for capturing seasonal and phenological traits of different LULC classes [20][21][22].

Hypsometry Analysis:

By examining grids of varied sizes over Digital Elevation Models (DEMs) with spatial resolutions of 90 meters and 30 meters, we were able to compute HI values for equal squares. The data set is available to the public from the Earth Remote Sensing Data Analysis Center (ERSDAC; www.gdem.aster.ersdac.or.jp) and serves as the source of the 30-meter resolution DEM offered through ERSDAC. The ASTER GDEM has a resolution of about 30 meters (1 arc second) and has been developed jointly by the US National Aeronautics and Space Administration (NASA) and the Ministry of Economy, Trade, and Industry of Japan (METI). The 90-m resolution DEM was created from NASA Shuttle Radar Topography Mission (SRTM, version 4) data at a 3 arc-second resolution. In comparison, the USGS releases such data for public use and can be accessed through not only the USGS FTP site but also the National Map Seamless Data Distribution System [23].

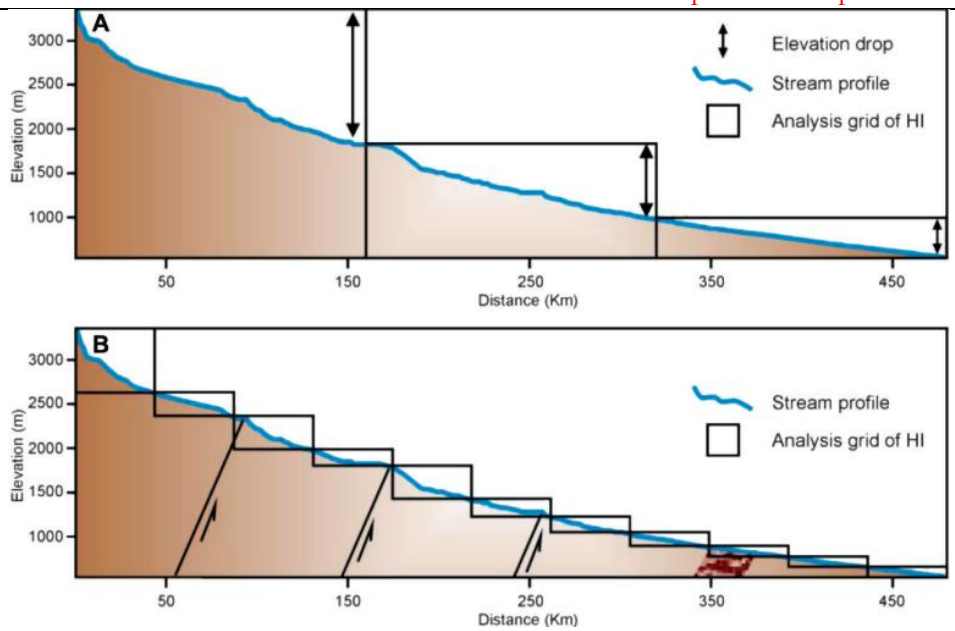

Figure 4. Dependence of Hypsometric Integral (HI) on Space [24]

It is stated that the Digital Elevation Model's (DEM) vertical inaccuracy is less than 16 meters. This DEM, which covers the majority of the planet, is reliable and accurate [25]. We calculated the mean, minimum, and maximum elevations over the DEMs using zonal statistics, allowing us to get each square's HI values. The HI values show notable differences across squares that are close to lithologic or tectonic boundaries. Owing to the intricacy of landscape dissection, high and low HI values may coexist depending on how the squares are allocated. HI distributions often exhibit a broad regional pattern with high and low HI values when tectonic forces are dominant [26]. According to [7], the HI is an index that describes how elevation is distributed in a certain geographic region, especially a drainage basin. The index represents the volume of a basin that has not been eroded and is defined as the region below the hypsometric curve (Figure).

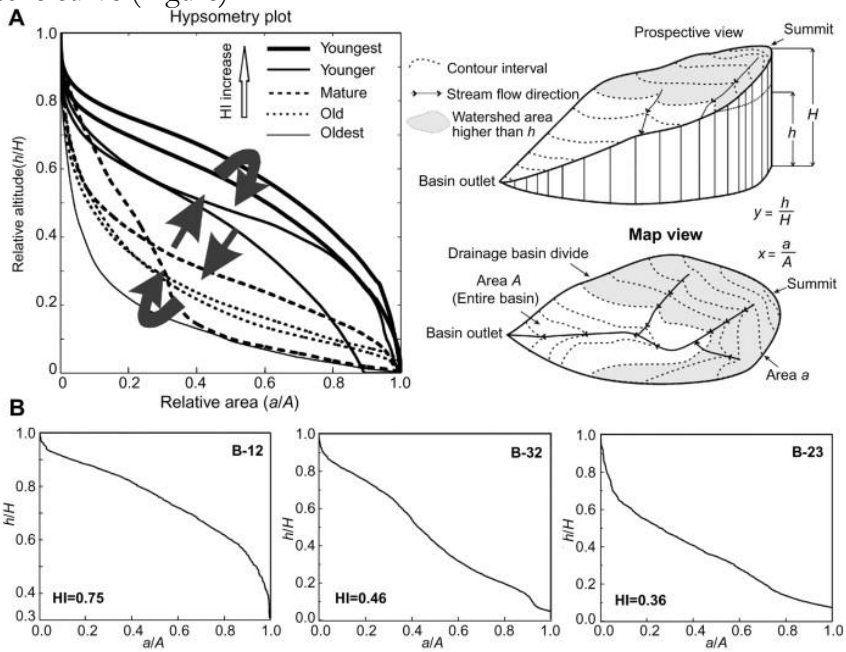

Figure 5. Schematic Diagram showing Mechanism of Hypsometric curves and Hypsometric integral computations [24]

Results and Discussion:

The RUSLE model, GIS, and remote sensing techniques have all been smoothly incorporated into the current study through the use of an integrated methodology. The Ghizer district's soil erosion danger zones were identified and mapped thanks to the method's synergistic computation of mean annual soil loss rates on a cell-by-cell basis. A wide range of data sources was used to develop the RUSLE model's parameters, all of which added to our understanding of erosion processes. The resulting maps of these RUSLE characteristics were carefully created and thoroughly investigated, shedding light on the many facets of soil erosion trends throughout the research region.

Rainfall Erosivity Factor (R):

The R factor, which expresses the amount of erosion caused by rainfall in millimeters per year, was recalculated using Google Earth Engine's revised erosivity formula. Next, using ArcGIS 10.8, an R factor map of the research region was made. As seen in the figure, the resultant R factor values for the study region vary from 130 to 966 mm/year.

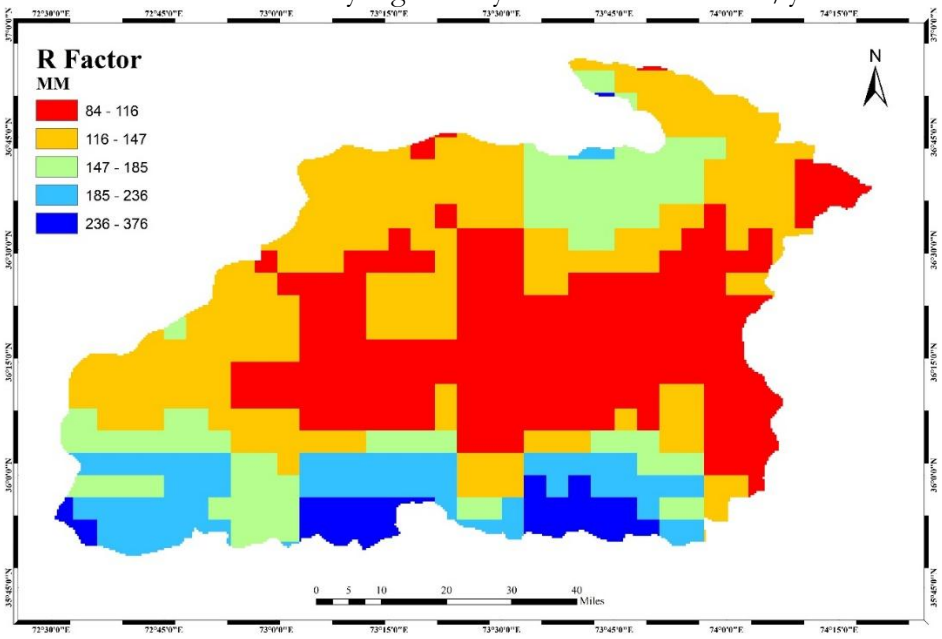

Figure 6. The research area's rainfall erosivity factor (R factor) map

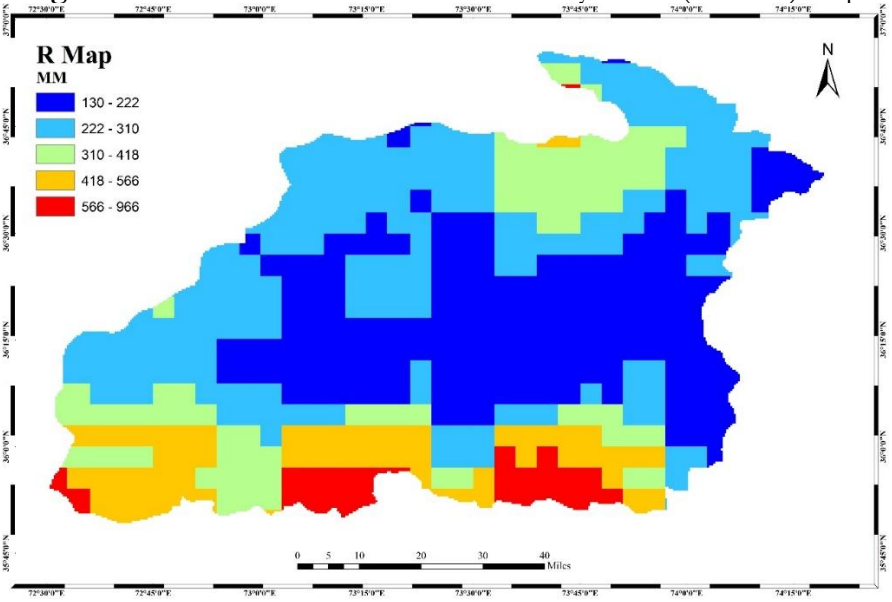

Figure 7. The area's R map

Soil Erodibility Factor (K):

In the research region, the K factor erodibility ranges from 0 to 0.05. Nonetheless, as Fig. shows, the bulk of the watershed is located between 0.03 and 0.05. As a result, a sizable section of the research area is vulnerable to erosion.

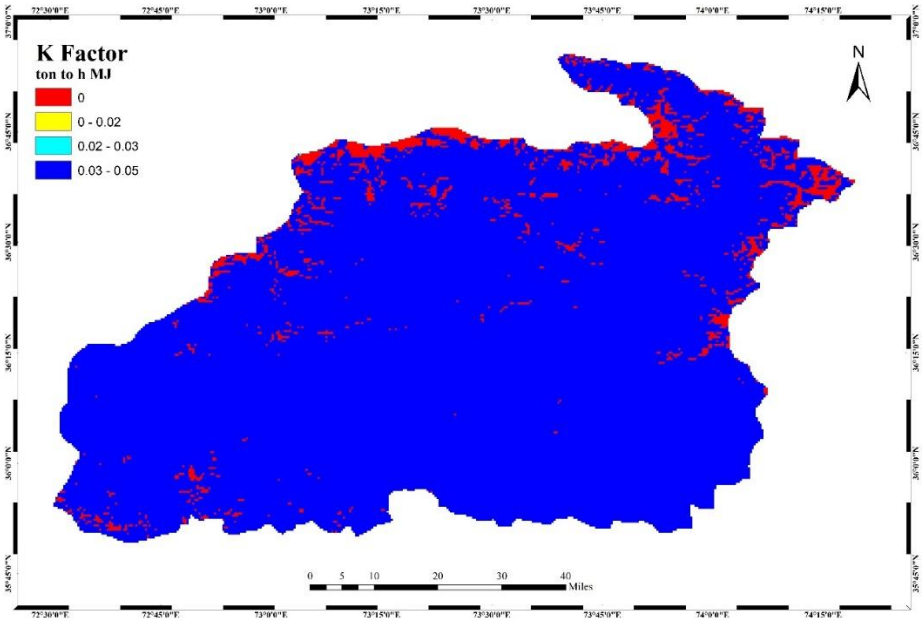

Figure 8. The research area's soil erodibility factor (K factor) map

Topographic factor (LS):

Based on the slope length and slope steepness analysis depicted in the figures, it has been observed that the northeastern and northwestern regions of the study area have an LS factor ranging from 937 to 4421, indicating higher steepness. In contrast, the rest of the study area exhibits less steep slopes, with the LS factor not exceeding 261.

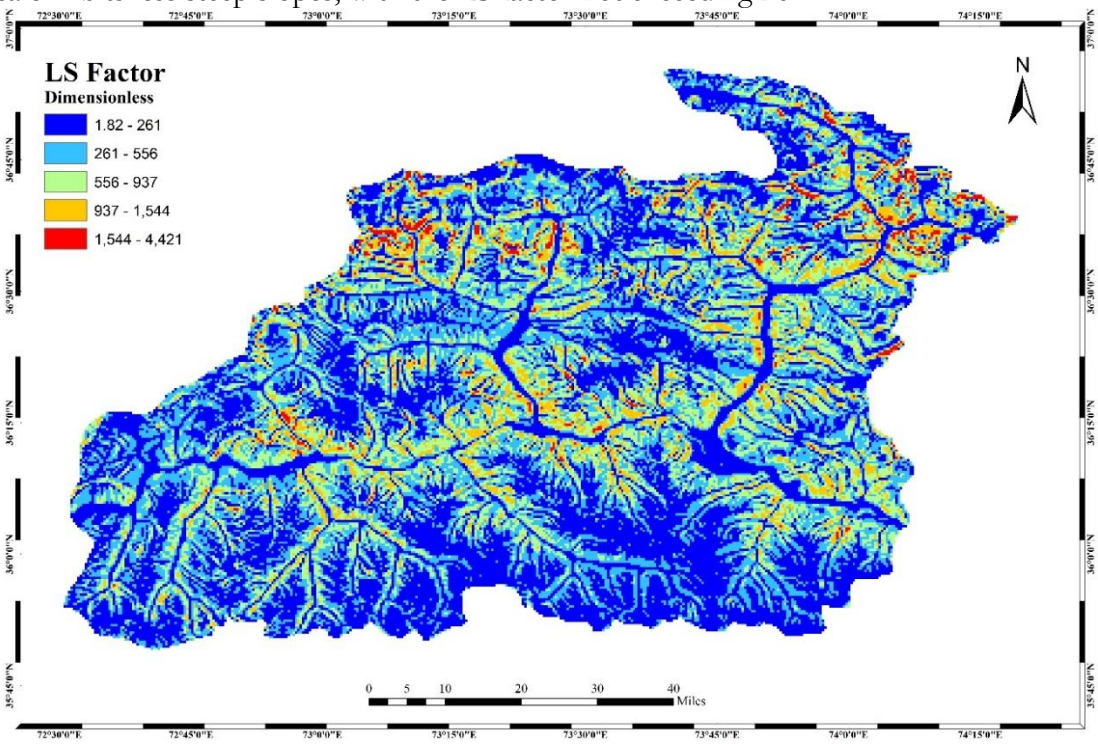

Figure 9. Research area's topographic factor (LS factor) map

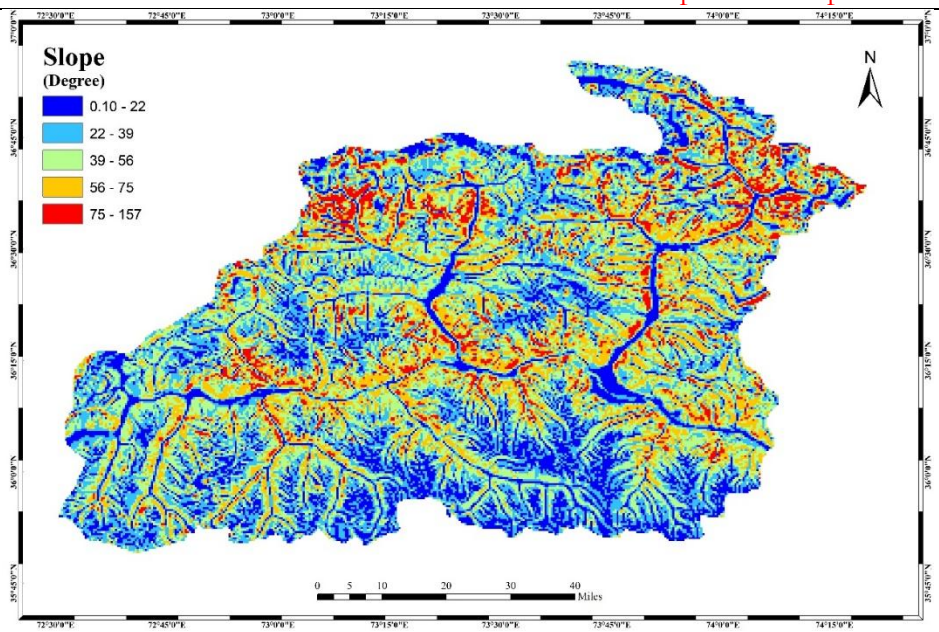

Figure 10. Study area's Slope map (in degrees)

Cover Factor (C):

Despite being a crucial statistic for crop management, the C factor is not easily accessible for the majority of crops grown in Pakistan. This component shows how various crops and management techniques affect the rates of soil erosion. The season and crop production method have an impact on how well vegetation and soil cover reduce erosion. The C factor has a value between 0.30 and 0.83. The cover factor map is shown in the image below.

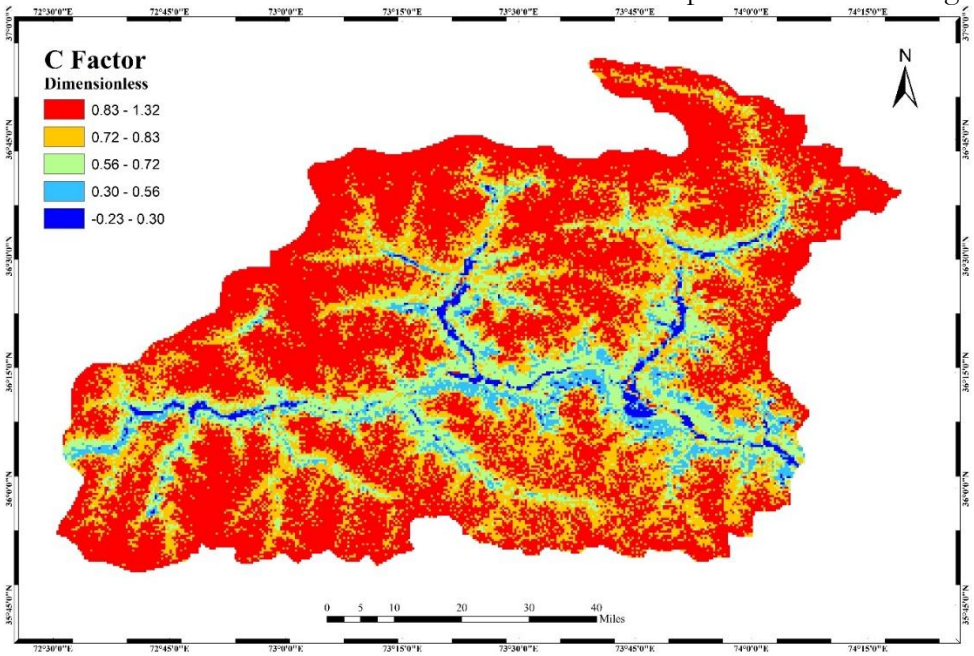

Figure 11. Cover factor (C factor) map for the area of study

Support Practice Factor (P):

The bulk of the region in the graphic indicates that the P factor for this study has a value between 0.5 and 1. The Agricultural Land Association states that the support practice factor often falls between 0 and 1. The fact that the number in this instance is closer to the higher end of the range indicates that conservation efforts are insufficient. To stop soil erosion, the terrain's surface is prepared.

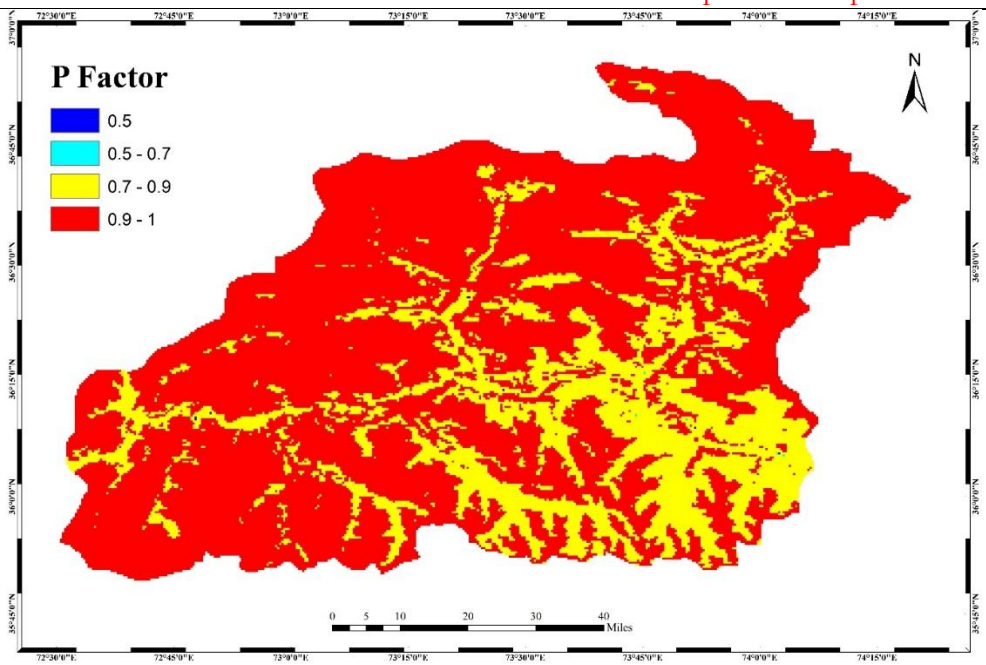

Figure 12. The study area's support practice factor (P factor) map

Soil Loss Map:

ArcGIS 10.8 and Google Earth Engine (GEE) were used to perform the erosion risk assessment for the Ghizer district. This was a geographical study including the overlaying of maps containing the five RUSLE components. Values between -342 and 24,199 were obtained by applying natural break categorization to the soil erosion intensity map. The Ghizer district's northeastern and northwest regions have the highest rates of erosion, as seen in the figure below. Significant quantitative insights into the kind, intensity, and geographic distribution of soil erosion were obtained using the RUSLE technique. It also made it easier to determine which regions were more impacted and what kinds of erosion predominated over time. As a result, RUSLE is a crucial instrument for managing soil erosion and facilitating the production of intricate quantitative maps.

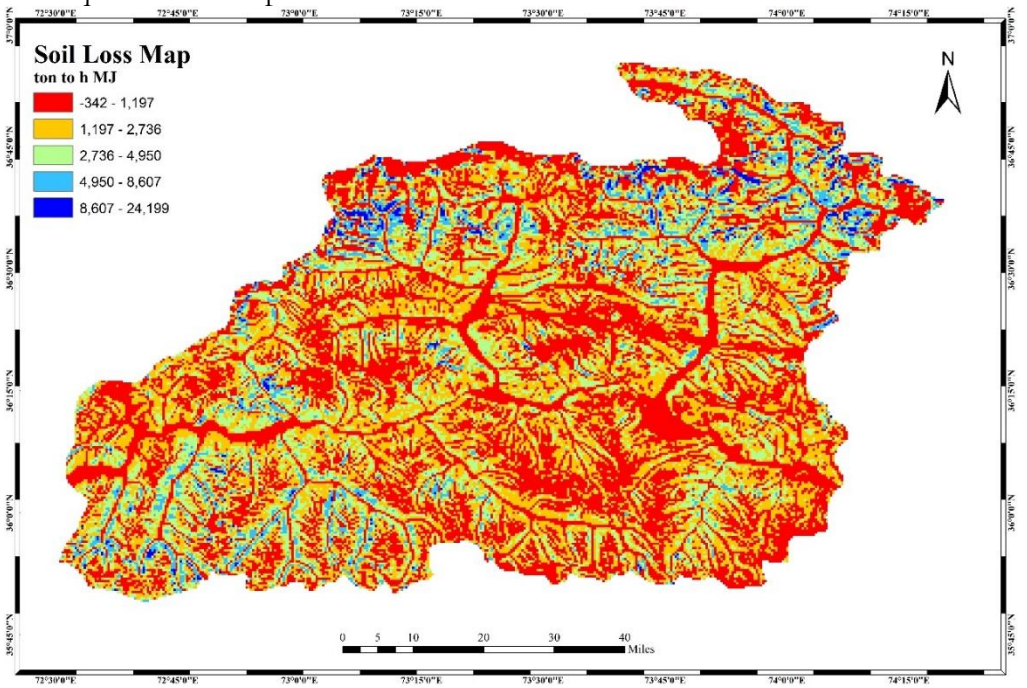

Figure 13. Soil Loss map of the research area

Hypsometric Analysis:

The rate of uplift for topographic changes throughout the research region and all facets of geological processes is determined by the hack gradient index and geomorphic indices. For each of the Ghizer basin's drainage linkages, the steepness and concavity are calculated using the incision detachment model and stream profile analysis. The steepness index values are calculated using the stream profile model, and the slopes across long spans are calculated using the regression model. Non-equilibrated profiles have knick-points; some of these knick-points are glided as a result of water channels being cut and soft rock components being eroded. The Ghizer Basin's concavity index map accurately depicts the whole area, showing that the bend in the river is caused by the presence of hard rocks beneath the surface, while the sections with soft rocks have seen greater erosion. The region's irregular topographical variations are a certain sign of tectonic activity, which indicates that the region's current rock structure is in an immature stage. Ghizer syntax and nearby places have frequent steep slope fluctuations, which is a crucial indicator for identifying the locations with the greatest relative uplift. The whole topography has been moved several kilometers away by one of the primary shear zones.

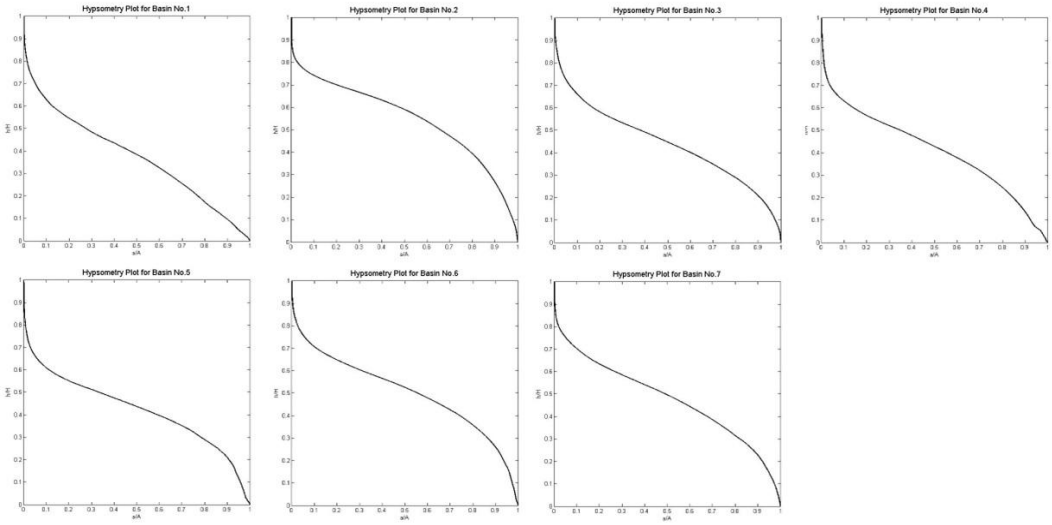

Figure 14. Hypsometric plots for the Strahler order 6th sub-basins Showing area-altitude relation in terms of erosion/uplift.

Conclusion:

An integrated methodology that included the RUSLE model, GIS, and remote sensing techniques was employed to analyze soil erosion in the Ghizer district. The results of this assessment have yielded important insights into the erosion dynamics of the region. The analysis emphasizes how soil erosion increased dramatically in the 20th century. In the Ghizer region, the RUSLE model, which was initially created for temperate climates but was modified for tropical ones, proved useful for calculating the rates of soil erosion in a variety of landforms and land use scenarios. Our results highlight the influence of topographic features, cover management, rainfall erosivity, soil erodibility, and support measures on soil erosion rates. The district's steep slopes and increased susceptibility to rainfall in the northeast and northwest areas resulted in the greatest rates of soil erosion. The higher values of the support practice component (P) in the study also demonstrated how inadequate the existing conservation efforts are. The Ghizer district's geomorphological characteristics were further contextualized by hypsometric analysis, which also revealed the spread of high-altitude terrain and intricate valley networks sculpted by glacial and river processes. A thorough knowledge of the erosion patterns and the impact of tectonic and lithologic limits on the landscape was made possible by the combination of DEM data with spatial autocorrelation analysis. To reduce soil erosion,

this research highlights the vital necessity for focused soil management and conservation measures, especially in areas with steep slopes and significant rainfall erosivity. The RUSLE model generates precise quantitative maps that land managers and policymakers may use to prioritize conservation efforts and put into practice efficient soil erosion control methods. The Ghizer district and comparable areas find that the RUSLE model, in conjunction with hypsometric analysis, is an invaluable resource for sustainable land management and soil protection.

Reference:

[1] E. M. Bridges, "World map of the status of humaninduced soil degradation, oldeman, L. R., Hakkeling, R. T. A. and Sombroek, W. G. UNEP/ISRIC, Nairobi, Kenya, 1990. isbn 90 6672 042 5, US$25.00 (paperback), 3 maps and explanatory note + 27 pp.," *L. Degrad. Dev.*, vol. 3, no. 1, pp. 68–69, Apr. 1992, doi: 10.1002/LDR.3400030109.

[2] B. P. Ganasri and H. Ramesh, "Assessment of soil erosion by RUSLE model using remote sensing and GIS - A case study of Nethravathi Basin," *Geosci. Front.*, vol. 7, no. 6, pp. 953–961, 2016, doi: https://doi.org/10.1016/j.gsf.2015.10.007.

[3] S. Q. Saifullah Khan, "Climate Change Impacts and Adaptation to flow of Swat River, Glaciers and Permafrost in Hindukush Ranges, Swat District, Pakistan (2004-2013)," International Journal of Economic and Environmental Geology. Accessed: Dec. 24, 2025. [Online]. Available: https://www.researchgate.net/publication/308032081_Climate_Change_Impacts_and_Adaptation_to_flow_of_Swat_River_Glaciers_and_Permafrost_in_Hindukush_Ranges_Swat_District_Pakistan_2004-2013

[4] S. Dutta, "Soil erosion, sediment yield and sedimentation of reservoir: a review," *Model. Earth Syst. Environ.*, vol. 2, 2016, [Online]. Available: https://link.springer.com/article/10.1007/s40808-016-0182-y

[5] W. M. M. V. M. Castillo, "Effectiveness and geomorphological impacts of check dams for soil erosion control in a semiarid Mediterranean catchment: El Cárcavo (Murcia, Spain)," *CATENA*, vol. 70, no. 3, pp. 416–427, 2007, doi: https://doi.org/10.1016/j.catena.2006.11.009.

[6] D. E. S. S. D. Angima, "Soil erosion prediction using RUSLE for central Kenyan highland conditions," *Agric. Ecosyst. Environ.*, vol. 97, no. 1–3, pp. 295–308, 2003, doi: https://doi.org/10.1016/S0167-8809(03)00011-2.

[7] A. N. Strahler, "Hypsometric (area-altitude) analysis of erosional topography. | Semantic Scholar," Geological Society of America Bulletin. Accessed: Dec. 24, 2025. [Online]. Available: https://www.semanticscholar.org/paper/Hypsometric-(area-altitude)-analysis-of-erosional-Strahler/d1b43da79631c6aa37281e2308d365b6276d9232

[8] David R. Montgomery; Greg Balco; Sean D. Willett, "Climate, tectonics, and the morphology of the Andes | Geology | GeoScienceWorld," geology. Accessed: Dec. 24, 2025. [Online]. Available: https://pubs.geoscienceworld.org/gsa/geology/article-abstract/29/7/579/188775/Climate-tectonics-and-the-morphology-of-the-Andes?redirectedFrom=fulltext

[9] S. H. Brocklehurst and K. X. Whipple, "Hypsometry of glaciated landscapes," *Earth Surf. Process. Landforms*, vol. 29, no. 7, pp. 907–926, Jul. 2004, doi: 10.1002/ESP.1083;ISSUE:ISSUE:DOI.

[10] R. C. Walcott and M.A. Summerfield, "Scale dependence of hypsometric integrals: An analysis of southeast African basins," vol. 96, no. 1–2, pp. 174–186, 2008, doi: https://doi.org/10.1016/j.geomorph.2007.08.001.

[11] J. M. A. J. V. Pérez-Peña, "CalHypso: An ArcGIS extension to calculate hypsometric

curves and their statistical moments. Applications to drainage basin analysis in SE Spain," *Comput. Geosci.*, vol. 35, no. 6, pp. 1214–1223, 2009, doi: https://doi.org/10.1016/j.cageo.2008.06.006.

[12] V. K. Pedersen and S. B. N. , D.L. Egholm, "Alpine glacial topography and the rate of rock column uplift: a global perspective," *Geomorphology*, vol. 122, no. 1–2, pp. 129–139, 2010, doi: https://doi.org/10.1016/j.geomorph.2010.06.005.

[13] F. H. P. Sternai, "Hypsometric analysis to identify spatially variable glacial erosion," *J. Geophys. Res. Earth Surf.*, 2011, doi: https://doi.org/10.1029/2010JF001823.

[14] RICHARD J PIKE; STEPHEN E WILSON, "Elevation-Relief Ratio, Hypsometric Integral, and Geomorphic Area-Altitude Analysis | GSA Bulletin | GeoScienceWorld," GSA Bulletin . Accessed: Dec. 24, 2025. [Online]. Available: https://pubs.geoscienceworld.org/gsa/gsabulletin/article-abstract/82/4/1079/7165/Elevation-Relief-Ratio-Hypsometric-Integral-and?redirectedFrom=fulltext

[15] J.-P. A. J.-E. Hurtrez, F. Lucazeau, J. Lavé, "Investigation of the relationships between basin morphology, tectonic uplift, and denudation from the study of an active fold belt in the Siwalik Hills, central Nepal," *J. Geophys. Res. Solid Earth*, 1999, doi: https://doi.org/10.1029/1998JB900098.

[16] S. Hussain, S. Hongxing, M. Ali, and M. Ali, "PS-InSAR based validated landslide susceptibility modelling: a case study of Ghizer valley, Northern Pakistan," *Geocarto Int.*, vol. 37, no. 13, pp. 3941–3962, 2022, doi: 10.1080/10106049.2020.1870165;REQUESTEDJOURNAL:JOURNAL:TGEI20;CTYPE:STRING:JOURNAL.

[17] K. H. Jodhani, D. Patel, N. Madhavan, and S. K. Singh, "Soil Erosion Assessment by RUSLE, Google Earth Engine, and Geospatial Techniques over Rel River Watershed, Gujarat, India," *Water Conserv. Sci. Eng.*, vol. 8, no. 1, pp. 1–17, Dec. 2023, doi: 10.1007/S41101-023-00223-X/METRICS.

[18] H. K. P. Vishal Kumar Singh, "Groundwater storage change estimation using GRACE data and Google Earth Engine: A basin scale study," *Phys. Chem. Earth, Parts A/B/C*, vol. 129, p. 103297, 2023, doi: https://doi.org/10.1016/j.pce.2022.103297.

[19] T. Desale, G. Metaferia, E. Shifaw, S. Abebe, W. Molla, and M. Asmare, "Identification and Prioritization of Sub-watersheds to Soil Erosion and Sediment Yield Susceptibility Using RUSLE, Remote Sensing, and GIS (Case Study: Abbay—Awash Basin in Wollo Area, Ethiopia)," *Water Conserv. Sci. Eng. 2023 81*, vol. 8, no. 1, pp. 1-, Jan. 2023, doi: 10.1007/S41101-023-00179-Y.

[20] Z. G. Shuang Liang, "Accurate Monitoring of Submerged Aquatic Vegetation in a Macrophytic Lake Using Time-Series Sentinel-2 Images," *Remote Sens.*, vol. 4, no. 3, p. 640, 20221, doi: https://doi.org/10.3390/rs14030640.

[21] X. Z. Chong Luo, "Regional soil organic matter mapping models based on the optimal time window, feature selection algorithm and Google Earth Engine," *Soil Tillage Res.*, vol. 219, p. 105325, 2022, doi: https://doi.org/10.1016/j.still.2022.105325.

[22] Z. Z. Qiang Zhou, "A novel regression method for harmonic analysis of time series," *ISPRS J. Photogramm. Remote Sens.*, vol. 185, pp. 48–61, 2022, doi: https://doi.org/10.1016/j.isprsjprs.2022.01.006.

[23] "Hole-filled seamless SRTM data V4. Tech. rep., International Centre for Tropical Agriculture (CIAT)." Accessed: Dec. 24, 2025. [Online]. Available: https://www.researchgate.net/publication/225091458_Hole-filled_seamless_SRTM_data_V4_Tech_rep_International_Centre_for_Tropical_Agriculture_CIAT

[24] S. Mahmood and R. Gloaguen, "Analyzing Spatial Autocorrelation for the Hypsometric Integral to Discriminate Neotectonics and Lithologies Using DEMs and GIS," *http://dx.doi.org/10.2747/1548-1603.48.4.541*, vol. 48, no. 4, pp. 541–565, Oct. 2013, doi: 10.2747/1548-1603.48.4.541.

[25] J. R. Samuel Blanchard, "Geomorphic Change Analysis Using ASTER and SRTM Digital Elevation Models in Central Massachusetts, USA," *GIScience Remote Sens.*, vol. 47, no. 1, 2010, doi: https://doi.org/10.2747/1548-1603.47.1.1.

[26] F. G.-L. J. V. Pérez-Peña, J. M. Azañón, A. Azor, J. Delgado, "Spatial analysis of stream power using GIS: SLk anomaly maps," *Earth Surf. Process. Landforms*, 2008, doi: https://doi.org/10.1002/esp.1684.

Copyright © by authors and 50Sea. This work is licensed under the Creative Commons Attribution 4.0 International License.